ATP Citrate Lyase: Activation and Therapeutic Implications in Non–Small Cell Lung Cancer

Toshiro Migita,[1] Tadahito Narita,[1,6] Kimie Nomura,[1] Erika Miyagi,[1] Fumika Inazuka,[1] Masaaki Matsuura,[2,3] Masaru Ushijima,[3] Tetsuo Mashima,[4] Hiroyuki Seimiya,[4] Yukitoshi Satoh,[5] Sakae Okumura,[5] Ken Nakagawa,[5] and Yuichi Ishikawa[1]

Divisions of [1]Pathology and [2]Cancer Genomics, The Cancer Institute, [3]Bioinformatics Group, Genome Center, [4]Division of Molecular Biotherapy, Cancer Chemotherapy Center, [5]Department of Thoracic Surgical Oncology, The Cancer Institute Hospital, Japanese Foundation for Cancer Research, and [6]Zenyaku Kogyo Co., Ltd., Tokyo, Japan

Abstract

Enhanced glucose and lipid metabolism is one of the most common properties of malignant cells. ATP citrate lyase (ACLY) is a key enzyme of *de novo* fatty acid synthesis responsible for generating cytosolic acetyl-CoA and oxaloacetate. To evaluate its role in lung cancer progression, we here analyzed ACLY expression in a subset of human lung adenocarcinoma cell lines and showed a relationship with the phosphatidyl-inositol-3 kinase–Akt pathway. The introduction of constitutively active Akt into cells enhanced the phosphorylation of ACLY, whereas dominant-negative Akt caused attenuation. In human lung adenocarcinoma samples, ACLY activity was found to be significantly higher than in normal lung tissue. Immunohistochemical analysis further showed phosphorylated ACLY overexpression in 162 tumors, well-correlating with stage, differentiation grade, and a poorer prognosis. Finally, to show the therapeutic potential and mechanism of ACLY inhibition for lung cancer treatment, we assessed the effect of RNA interference targeting ACLY on lipogenesis and cell proliferation in A549 cells. ACLY inhibition resulted in growth arrest *in vitro* and *in vivo*. Interestingly, increased intracellular lipids were found in ACLY knockdown cells, whereas *de novo* lipogenesis was inhibited. Supplementation of insulin could rescue the proliferative arrest elicited by ACLY inhibition; however, in contrast, fatty acid palmitate induced cell death. Taken together, these findings suggest that ACLY is involved in lung cancer pathogenesis associated with metabolic abnormality and might offer a novel therapeutic target. [Cancer Res 2008;68(20):8547–54]

Introduction

One of the most common properties of cancer cells is a metabolic change into high glycolysis and lipogenesis to satisfy the increased demand for energy and macromolecules need for autonomous growth. It is assumed that phosphatidyl-inositol-3 kinase (PI3K)-Akt signaling pathway plays a part in this phenomenon, and constitutive activation of this pathway is frequently observed in many types of cancers. Proto-oncogene Akt, downstream from PI3K, exhibits oncogenic effects with influence on proliferation, survival, motility, and morphology. Akt also plays a pivotal role of cancer metabolism via the stimulation of nutrient uptake, glycolysis, and fatty acid biosynthesis through action on glucose transporters, glycolytic enzymes, and lipogenic enzymes (1–3).

Accumulating evidence indicates that dysregulated glycolysis and lipid synthesis contribute to cancer pathogenesis. Fluorodeoxyglucose- or ^{11}C-acetate–positron emission tomography imaging based on the metabolic difference between normal and neoplastic tissue is useful in cancer detection (4, 5). Thus, glucose and lipid metabolism–targeting therapeutics have attracted great attention (6–8). Inhibitors of hexokinase have been shown to reduce ATP concentrations leading to cytotoxicity in tumor cells (9). Also, inhibitors of lipid synthesis such as statins, farnesyl transferase inhibitors, and fatty acid synthase (FASN) inhibitors impair proliferation or induce apoptosis of tumor cells (7, 10).

ATP citrate lyase (ACLY) is a key enzyme of *de novo* fatty acid synthesis. ACLY is involved in the generation of cytosolic acetyl-CoA and oxaloacetate from citrate and, thus, contributes to the translocation of acetyl-CoA from mitochondria to cytosol. It has been found that Akt directly phosphorylates and activates ACLY (11). More recently, it has been reported that chemical inhibitors or ACLY RNAi suppress tumor cell growth (12, 13). Because ACLY functions depend on glucose utility and its product acetyl-CoA is a building block for cholesterol and fatty acid synthesis, ACLY must play a crucial role in cancer cell metabolism.

Lung cancer is the leading cause of cancer death in the worldwide and is a typical tumor displaying a high rate of glycolysis and fatty acid synthesis. Thus, targeting dysregulated metabolism may be an attractive strategy for lung cancer treatment.

In this study, we therefore examined the contribution of ACLY to lung cancer pathogenesis and its therapeutic potential. Overexpression and activation of ACLY in patients with lung adenocarcinoma could be shown, and it was found to be a statistically significant negative prognostic factor. Selective ACLY inhibition resulted in the inhibition of tumor cell growth *in vitro* and *in vivo*. Growth arrest induced by ACLY inhibition was associated with intracellular lipid accumulation, despite of the inhibition of *de novo* lipogenesis. Our findings suggest that ACLY plays a critical role in cancer progression and metabolic changes, and may be a promising therapeutic target in lung cancer.

Materials and Methods

Cell culture and clinical samples. The human lung adenocarcinoma cell lines A549, NCI-H460, NCI-H23, NCI-H522, HOP62, COR-L105, and PC14 were obtained from the American Type Culture Collection and grown in RPMI 1640 supplemented with 10% fetal bovine serum (both medium and serum from Life Technologies Bethesda Research Laboratories) and 1% penicillin/streptomycin in an atmosphere of 5% CO_2 at 37°C.

Requests for reprints: Toshiro Migita, Division of Pathology, The Cancer Institute of Japanese Foundation for Cancer Research, 3-10-6, Ariake, Koto-ku, Tokyo, Japan, 135-8550. Phone: 3-3520-0111; Fax: 3-3570-0558; E-mail: toshiro.migita@jfcr.or.jp.

doi:10.1158/0008-5472.CAN-08-1235

We also analyzed lung cancer tissue from operable patients that had developed lung adenocarcinoma. All tumors were pathologically diagnosed based on the WHO classification of lung tumors (14) and staged according to the classification of the Union Internationale Contre le Cancer. Data for clinicopathologic variables and patient prognosis were also obtained. All experiments were performed using a protocol approved by the Institutional Review Board of the Japanese Foundation for Cancer Research (#2007-1058).

Transient transfections. Constitutively active myristolated Akt and the dominant-negative Akt plasmids were generous gifts from Dr. Yukiko Gotoh (Institute of Molecular and Cellular Biosciences, University of Tokyo, Japan). Cells were plated at 7×10^5 per well in 60-mm dishes and transfected in triplicate using the FuGENE 6 Transfection Reagent according to the manufacturers protocol (Roche Diagnostics, Inc.). Experiments were repeated at least thrice.

RNA preparation and reverse transcription-PCR. The cell lines in logarithmic phase of growth and the frozen tissue samples were collected for RNA extraction, using an RNeasy kit (Qiagen) and total RNA was applied for first-strand cDNA synthesis with a high-capacity cDNA Reverse Transcriptase kit (Applied Biosystems). Gene-specific probes and primer were obtained from Universal ProbeLibrary (Roche Applied Science) and primer sequences were as follows: 5′-gaagggagtgaccatcatcg-3′ (ACLY forward); 5′-ttaaagcacccaggcttgat-3′ (ACLY reverse); 5′-gctcctccatcaatgacaaaa-3′ (SREBP-1 forward); 5′-tgcgcaagacagcagattta-3′ (SREBP-1 reverse). PCR was carried out in 96-well plates using the LightCycler 480 System (Roche Applied Science). All reactions were performed at least in triplicate. The relative amounts of all mRNAs were calculated using the comparative computed tomography method after normalization to human β-2-microglobulin (B2M) for human samples. Semiquantitative reverse transcription-PCR (RT-PCR) was carried out using SYBR Green for the cell lines. β-actin was used as an internal control.

Cell lysis and immunoblotting. To obtain total protein lysates, frozen tissue and cells were homogenized and dissolved in radioimmunoprecipitation assay buffer [150 mmol/L NaCl, 1.0% Igepal CA-630, 0.5% sodium deoxycholate, 0.1% SDS, 50 mmol/L Tris (pH 8.0); Sigma] containing proteinase inhibitors and phosphatase inhibitors. The protein concentration of each lysate was determined using a protein assay reagent kit (Bio-Rad). The total cell lysate was applied on 10% SDS-PAGE. After electrophoresis, the proteins were transferred electrophoretically from the gel to polyvinylidene difluoride membranes (Millipore). The membranes were then blocked for 1 h in blocking buffer (5% low-fat dried milk in TBS) and probed with the primary antibodies overnight. After being washed, the protein content was made visible with horseradish peroxidase–conjugated secondary antibodies followed by enhanced chemiluminescence (Amersham). The primary antibodies used were raised against phosphorylated ACLY (Ser 454), total ACLY, phosphorylated Akt (Ser 473), total Akt, phosphorylated Erk1/2 (Thr 202/Tyr 204), PTEN (all obtained from Cell Signaling Technology), SREBP-1 (BD Bioscience), and β-actin (Sigma). LY294002 and wortmannin were purchased from Sigma.

ACLY activity. ACLY activity was measured via the malate dehydrogenase–coupled method (15). Total protein lysates extracted from cell lines or clinical samples were subjected to the assay. Change in absorbance in the absence of exogenous ATP was subtracted from change in the presence of ATP and was normalized to protein concentration to determine the specific ACLY activity.

RNA interference. siRNA oligonucleotides for ACLY and a negative control were purchased from Invitrogen. Three independent oligonucleotides were used for ACLY siRNA. The ACLY siRNA#1 sequence was 5′-UUCUUGAUCAGCUUUCUCGUGAGGG-3′. The others were designed to correspond to a previous report (13). Transfection was performed using Lipofectamine RNAiMAX (Invitrogen) according to the manufacturer's protocol. Briefly, 60 pmol of siRNA and 10 μL of Lipofectamine RNAiMAX were mixed in 1 mL of Opti-MEM medium (10 nmol/L final siRNA concentration). After 20 min of incubation, the mixture was added to the suspended cells and these were plated on dishes for each assay. Seventy-two hours after transfection, cells were analyzed for all experiments.

Flow cytometry. For determination of the cell cycle distribution after siRNA treatment, DNA content was measured by flow cytometry with propidium iodide (PI). Briefly, 72 h after siRNA treatment on 60-mm dishes, the cells were harvested and cell pellets were then fixed with 70% ethanol. Cells were incubated with 20 μg/mL RNase A at 37°C for 30 min and then stained with 10 μg/mL PI. The cell cycle distribution was acquired with a FACScalibur (Becton Dickinson), and the percentage of cells in each phase of the cell cycle was analyzed with ModFit software.

Assessment of cell proliferation and cell death. Cells (5×10^4 cells per mL) were transfected with siRNA and placed in a 96-well culture plate on day 0. On day 2, vehicle or 20 μg/mL insulin (Life Technologies Bethesda Research Laboratories) or 100 μmol/L palmitate (Sigma) was added to the medium. On day 3, cell proliferation, as measured as the number of viable cells, was evaluated at 450 nm absorbance using Cell Count reagent SF (Nacalai Tesque). The cell death rate (% of total population) was also determined by trypan blue exclusion assay. Palmitate-bovine serum albumin (BSA) complex was prepared according to the previous report (16).

Lipid synthesis. A549 cells were transfected with siRNA and were plated onto 60-mm dishes. After culturing for 72 h, the cells were incubated in the medium containing 4 μCi/mL D-[6-^{14}C]glucose (GE Healthcare) for 4 h. Cellular lipids were extracted by a Bligh Dyer method (17). The rate of conversion of glucose into lipid was evaluated as described (12). Assay was performed in triplicate, and the results were expressed as percentage change in cpm per mg protein.

Immunohistochemistry, immunocytochemistry, and lipid staining. Tissue microarrays (TMA) consisting of 162 cases of lung adenocarcinoma were constructed for immunohistochemistry (IHC). IHC was performed on 5-μm thick, formalin-fixed, paraffin-embedded sections using primary antibodies for p-ACLY (Ser 454) and p-AKT (Ser 473; purchased from Cell Signaling Technology). Antigen retrieval was performed for 30 min in citrate buffer for each antibody. The slides were developed using the labeled streptavidin biotinylated peroxidase method (Nichirei) according to the manufacturer's instructions. For p-Akt immunostaining, the Tyramide Signal Amplication System (CSA II; DakoCytomation) was used. 3,3′-Diaminobenzidine tetrahydro-chloride was used as the chromogen and hematoxylin as the counterstain. All immunohistochemical staining was accomplished with a Dako Autostainer (DakoCytomation) under the same conditions. The expression and staining intensity on TMAs were scored semiquantitatively without knowledge of patient identity or outcome: 0, no; 1, weak; 2, moderate; 3, moderate to strong; 4, strong and scores were averaged across three cores. Patients were classified into two groups: p-ACLY-low (score 0–2) and p-ACLY-high (score 3,4). p-Akt expression was also divided into two groups according to the ACLY classification.

For immunocytochemistry, the cells were fixed with 4% paraformaldehyde 72 h after transfection. After PBS washing and treatment with 0.2% Triton X-100, the cells were blocked using Protein Block (DakoCytomation) for 10 min at room temperature and then incubated with p-ACLY (Cell Signaling Technology) or total ACLY (C-20 and G-17; Santa Cruz) antibodies 4°C overnight. Cells were washed and then incubated with FITC-conjugated secondary antibodies (DakoCytomation) for 1 h at room temperature. Cells were washed in PBS, mounted, counterstained with 4′,6-diamidino-2-phenylindole dihydrochloride, and visualized with the fluorescence microscope (Olympus).

Intracellular lipid accumulation was detected by oil red O (Sigma) or HCS LipidTOX phospholipidosis and steatosis detection kit (Invitrogen) according to the manufacture's protocol.

***In vivo* siRNA treatment of xenograft.** Nude mice were inoculated with 1×10^6 A549 cells. The negative control or ACLY siRNA#1 (5 μmol/L) with 0.05% atelocollagen (Koken) in a 200-μL volume was injected s.c. around the tumor, according to the manufacture's instruction. Injection was performed at weekly intervals for 5 wk. Each experimental condition included 10 animals per group. Tumor dimensions and body weight were measured weekly and the tumor volumes calculated using the formula: $1/2\ a\ b^2$, where a and b represent the larger and smaller tumor diameters, respectively. At the end of the experiment, tumors were excised for histologic analysis.

Tumor samples were fixed in 20% formaldehyde-PBS(−) and embedded in paraffin for H&E staining and IHC. IHC was performed for expression of p-ACLY and Ki-67, a proliferation marker (DakoCytomation).

Table 1. Relationship between p-ACLY expression and clinicopathologic characteristics in lung adenocarcinoma

	p-ACLY low, *n* (%)	p-ACLY high, *n* (%)	*P*
Age (y; average)	64	62.8	
Gender			
Male	34 (21.0)	46 (28.4)	0.1932
Female	26 (16.0)	56 (34.6)	
Smoking habit			
Never	25 (15.4)	49 (30.2)	0.514
Smoker	35 (21.6)	53 (32.7)	
Tumor size			
<30 mm	31 (19.1)	50 (30.9)	0.8708
>30 mm	29 (17.9)	52 (32.1)	
Stage			
I	44 (27.2)	51 (31.5)	<0.01
II–IV	16 (9.9)	51 (31.5)	
Pleural invasion			
Absence	44 (30.1)	47 (32.2)	<0.01
Presence	13 (8.9)	42 (28.8)	
Tumor differentiation			
Well	38 (23.5)	33 (20.4)	<0.001
Moderate	17 (10.5)	45 (27.8)	
Poor	5 (3.1)	24 (14.8)	
p-Akt expression			
Low	30 (18.5)	31 (19.1)	0.0184
High	30 (18.5)	71 (43.8)	

Statistical analysis. For *in vitro* experiments, statistical analysis was performed using Student's *t* tests. An exponential regression model was used for evaluation of *in vivo* experiment. Kaplan-Meier survival curves were constructed for patients with p-ACLY–low and p-ACLY–high expression, and differences between survival curves were tested by a multivariate Cox regression model. Fisher's exact tests for contingency tables were used in Table 1. For all analyses, *P* value of <0.05 was considered statistically significant. Statistical analyses were performed using statistical programming language of R (18) and STATISTIKA (Statsoft, Inc.).

Results

Positive correlation between p-Akt and p-ACLY expression levels in lung adenocarcinoma cell lines. To investigate ACLY

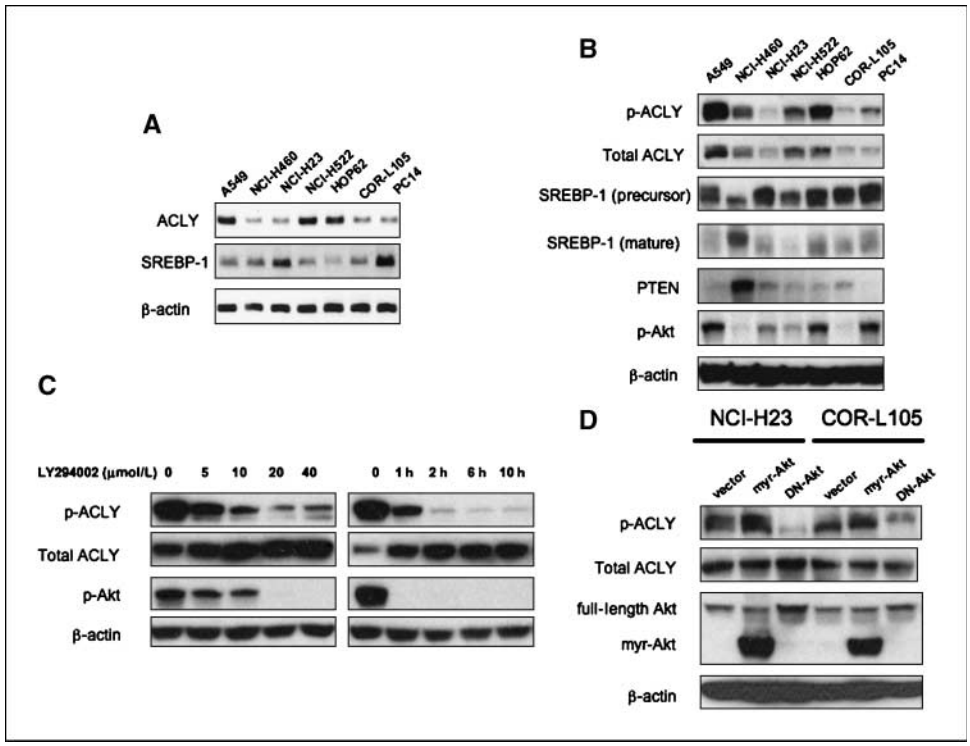

Figure 1. PI3K-Akt pathway is involved in ACLY phosphorylation. Equal cell numbers were plated in 60-mm dishes and allowed to attach for 24 h. *A,* semiquantitative RT-PCR for ACLY, SREBP-1, and β-actin (control) was performed in lung adenocarcinoma cell lines. *B,* immunoblotting was performed as described in the Materials and Methods. ACLY is highly phosphorylated in A549, HOP62, and PC14, having the highest levels of p-Akt. A representative data set from two independent experiments is shown. *C,* A549 cells were treated with the PI3K inhibitor LY294002 and Western blots were performed with a p-ACLY, total ACLY, p-Akt, and β-actin antibodies. *Left,* dose curve; cells were treated with increasing concentrations of LY294002 for 2 h; *Right,* time course; cells were treated with 20 μmol/L LY294002 for 1, 2, 6, 10 h. *D,* NCI-H23 and COR-L105 cells were transiently transfected with empty vector, constitutive active Akt (*myr-Akt*), or dominant negative Akt (*DN-Akt*). Samples were harvested for immunoblotting with anti–p-ACLY, total ACLY, p-Akt, and β-actin 48 h after transfection.

regulation, we assessed ACLY expression as well as a transcriptional factor SREBP-1 expression at both mRNA and protein levels in various human lung adenocarcinoma cell lines. ACLY was expressed in all cell lines, protein levels closely paralleling mRNA expression (Fig. 1*A* and *B*). SREBP-1 is a member of the basic helix-loop-helix-leucine zipper family of transcriptional factors that play a central role in the expression of lipogenic enzymes. However, our data showed the inverse relationship between ACLY and SREBP-1 mRNA levels (Fig. 1*A*). Moreover, total ACLY protein levels were independent of either the 125 kDa precursor form of SREBP-1 or the 60 to 70 kDa mature, cleaved form (Fig. 1*B*). These findings thus suggested that ACLY protein expression is regulated at the transcription level, however by an as yet unknown transcription factor other than SREBP-1.

Notably, phosphorylated ACLY levels were likely to follow total ACLY levels, suggesting ACLY phosphorylation contributes to its protein stabilization. Furthermore, the increase in ACLY phosphorylation status seemed to follow p-Akt levels in most cell lines (Fig. 1*B*). These findings suggest Akt contributes to stabilize ACLY protein by means of its phosphorylation. In addition, p-Erk1/2, a mitogen-activated protein kinase (MAPK), levels were not correlated with ACLY phosphorylation (data not shown).

ACLY phosphorylation is directly regulated by PI3K-Akt pathway. Next, we determined whether ACLY is a downstream target of the PI3K-Akt pathway in lung cancer. Treatment with LY294002 or wortmannin (data not shown), PI3K inhibitors, resulted in the decrease in ACLY phosphorylation in a dose- and time-dependent manner in A549 cells, in parallel with a dramatic decrease in Akt phosphorylation (Fig. 1*C*). In addition, U0126, a MAPK inhibitor, did not affect p-ACLY expression (data not shown). To determine whether Akt, a downstream effecter of PI3K, directly regulates ACLY phosphorylation, constitutively active Akt or dominant-negative Akt were introduced into NCI-H23 and COR-L105 cells. The introduction of constitutively active Akt into the cells resulted in the enhancement of ACLY phosphorylation, whereas the dominant negative Akt attenuated ACLY phosphorylation (Fig. 1*D*). Total ACLY levels were not changed substantially.

ACLY is activated and a prognostic factor in human lung adenocarcinomas. We then assessed ACLY expression and activity in human lung adenocarcinoma tissues. The average mRNA level of ACLY was up-regulated 2.1-fold compared with that in corresponding normal tissue samples ($P < 0.05$; Fig. 2*A*). Western blot also revealed p-ACLY levels to be much higher in lung adenocarcinomas than in background lung tissue, whereas total ACLY levels were slightly increased in lung adenocarcinoma (Fig. 2*B*). In spite of higher amounts of the precursor form of SREBP-1 in tumors, the levels of the mature form tended to be lower than in corresponding normal tissue (Fig. 2*B*). In line with expression analysis, ACLY activity was significantly higher in tumors compared with normal tissue ($P < 0.01$; Fig. 2*C*).

To identify associations with clinicopathologic variables, IHC for p-ACLY was performed on TMA. p-ACLY expression in tumor tissue

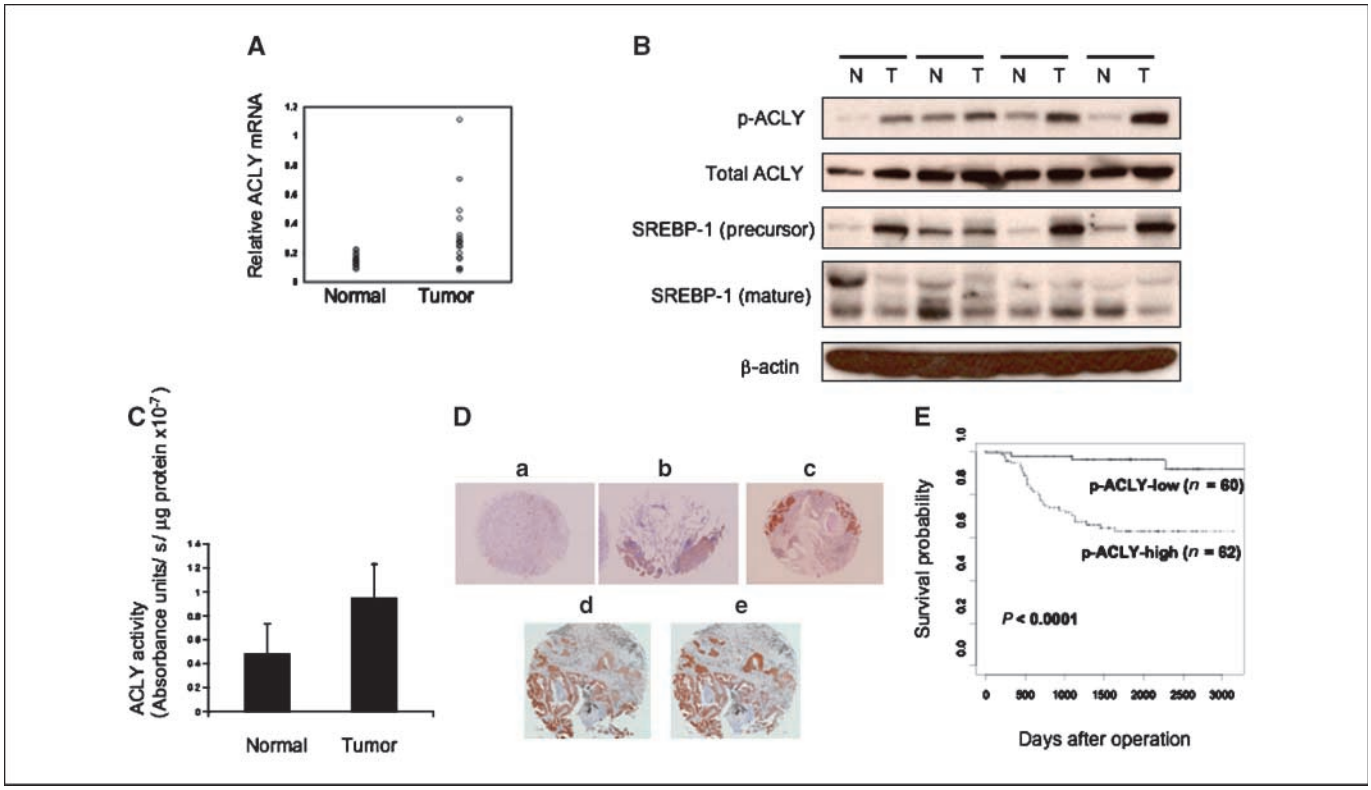

Figure 2. ACLY expression and activity in human lung adenocarcinoma samples. *A,* ACLY mRNA expression was measured in 17 human lung tumors and 16 normal tissue samples by quantitative RT-PCR. The mRNA levels of ACLY are presented as arbitrary units for the mRNA levels of B2M. *B,* representative immunoblot for p-ACLY and SREBP-1 in four pairs of frozen samples of lung tumors and normal tissue. *C,* ACLY activity is shown for 10 pairs of human lung tumors and normal tissue. *Columns,* mean; *bars,* SD. Statistical analyses were conducted with the *t* test (*A,* $P = 0.015$; *C,* $P = 0.0036$, respectively). *D,* representative pictures of various immunostaining patterns of p-ACLY (*a*, weak; *b*, moderate; *c*, strong), and p-Akt (*d*) and p-ACLY (*e*) expression in serial sections. *E,* overall survival of lung adenocarcinoma patients with reference to p-ACLY expression. Differences between the two groups were evaluated with the multivariate Cox regression model.

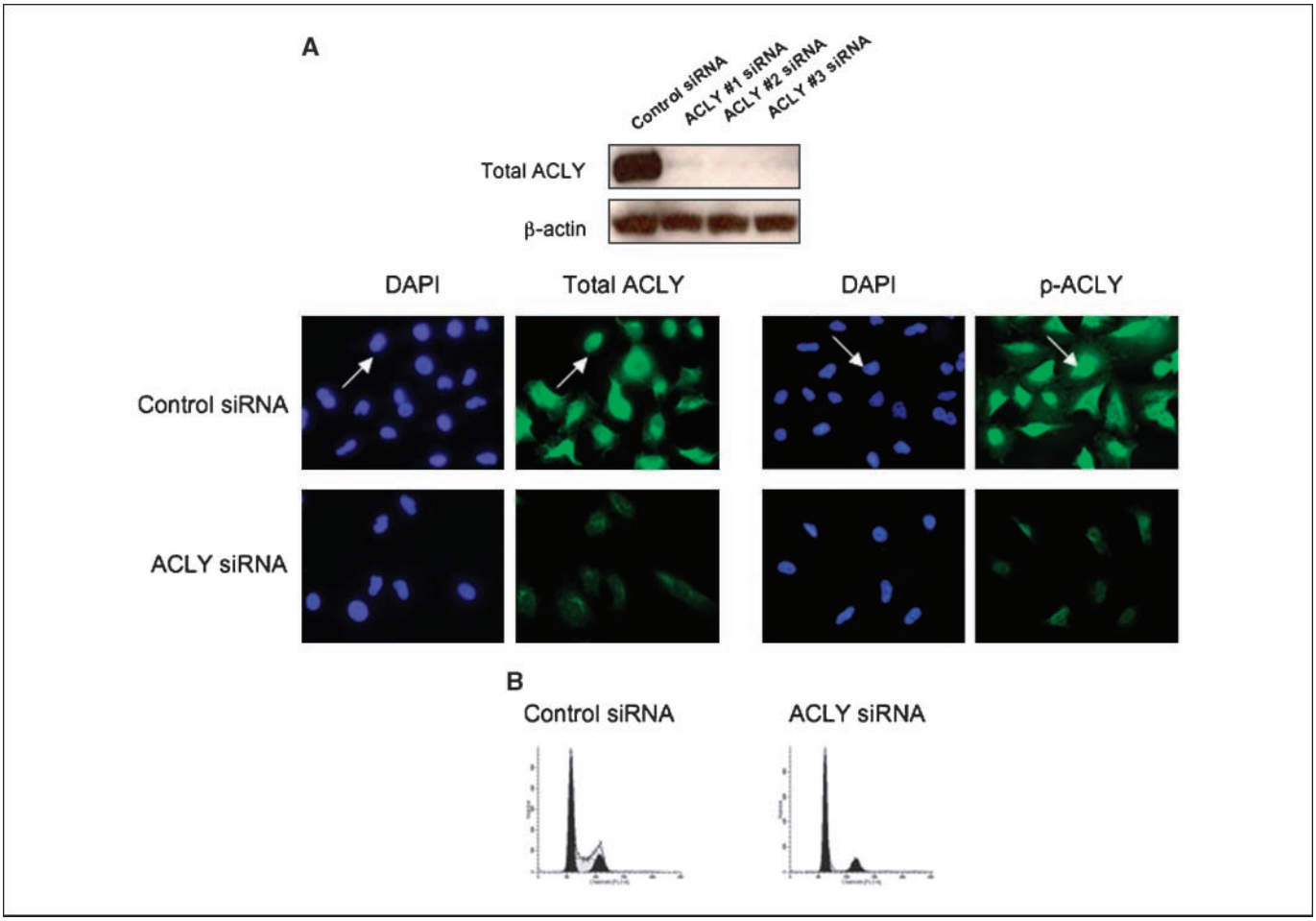

Figure 3. ACLY inhibition induces cell-cycle arrest in A549 cells *in vitro. A,* ACLY protein levels of A549 cells transfected with negative control siRNA or three different ACLY siRNA oligonucleotides were determined by Western blot analysis at 72 h after transfection. Immunocytochemistry was performed with the cells treated with negative control siRNA or ACLY siRNA #1 (unless otherwise noted) using total ACLY and p-ACLY antibodies. Both proteins were detected in the cytoplasm as well as in the nucleus (*arrows*). *B,* flow cytometry showing changes of cell-cycle phase distribution 72 h after siRNA treatment.

was detected in both cytoplasm and nucleus of tumor cells, whereas was barely detectable in the corresponding normal tissue. Among the 162 tumor samples, immunostaining intensity was variable (Fig. 2*D, a–c*). There was a strong p-ACLY expression in 63.0% (102 of 162) of patients with lung adenocarcinoma. Comparison between clinicopathologic variables and p-ACLY levels revealed that positivity for p-ACLY was significantly associated with advanced stage ($P < 0.01$), the presence of pleural invasion ($P < 0.01$), and poor differentiation ($P < 0.001$; Table 1). These findings suggest that high expression of p-ACLY could be generally related to aggressive biological behavior of lung cancer.

Cytosomal and/or nuclear staining of p-Akt was observed in 62.3% (101 of 162) of lung adenocarcinoma cases (Table 1), and we found that the p-Akt and p-ACLY immunostaining patterns well correlated (Table 1; Fig. 2*D, d* and *e*).

Next, we examined the relationship between expression of p-ACLY and survival in patients with lung adenocarcinoma ($n = 162$). The 5-year survival was 96.5% in patients with p-ACLY–low lung adenocarcinomas, whereas it was 63% in patients with p-ACLY–high lung adenocarcinomas ($P < 0.0001$; Fig. 2*E*). On univariate Cox regression analyses, stage, tumor size, pleural invasion, gender, tumor differentiation, and p-ACLY expression were significantly associated with survival ($P < 0.05$). Furthermore, in the multivariate model with these significant covariates, p-ACLY expression was a significant factor for prediction of a poor prognosis ($P = 0.0025$), together with stage and tumor size ($P = 0.00029$ and $P = 0.027$, respectively).

ACLY is a therapeutic target in non–small cell lung cancer. To determine whether ACLY is a therapeutic target in lung cancer, we analyzed the phenotype of A549 cells treated with ACLY inhibition. All three oligonucleotides of ACLY siRNA resulted in an efficient knockdown of total ACLY protein levels, as determined by Western blot and immunocytochemistry (Fig. 3*A*). Phoshophorylated and total ACLY proteins were localized in the cytoplasm as well as in the nucleus (Fig. 3*A, arrows*). Morphologically, ACLY knockdown was associated with curved, thinner, and elongated cells, in contrast to negative control siRNA. DNA flow cytometric analysis indicated that ACLY knockdown induced a progressive reduction in the S phase fraction associated with a progressive parallel accumulation of G_1 phase (control siRNA: G_1, 51.5%; S, 32.6%; G_2-M, 15.9%; ACLY siRNA: G_1, 79.0%; S, 4.0%; G_2-M, 17.1%; Fig. 3*B*). No significant increase of sub-G_1 cell population was observed at least 72 hours after ACLY knockdown. Microscopic observations of trypan blue staining revealed negligible cell death after ACLY knockdown (data not shown).

Next, to examine the effects of ACLY inhibition on lipogenesis and cell proliferation, we assessed ACLY activity, *de novo* fatty acid synthesis, intracellular lipid levels, and cell numbers. The treatment of LY294002 or ACLY knockdown resulted in a significant decrease in ACLY activity (Fig. 4*A, a*). As anticipated, the decreased conversion rate of glucose to lipid was observed after the treatment of LY294002 or ACLY knockdown (Fig. 4*A, b*), consistent with previous report (13). However, despite the impairment of *de novo* lipogenesis, lipidTOX, or oil red O (data not shown) staining revealed the markedly increased accumulation of phospholipids and neutral lipids in the cytoplasm after the ACLY knockdown (Fig. 4*A, c*). Cell proliferation was decreased significantly in the cells treated with LY294002 (data not shown) or ACLY siRNA compared with negative control siRNA (Fig. 4*B*). To examine whether the growth arrest induced by ACLY inhibition was related to the impairment of glucose or lipid metabolism, ACLY knockdown cells were exposed for 24 hours to exogenous insulin or palmitate. The supplementation of insulin improved cell proliferation when compared with ACLY siRNA alone ($P < 0.005$; Fig. 4*B*), whereas palmitate markedly suppressed cell proliferation accompanied by cell death ($P < 0.001$; Fig. 4*B*).

Finally, to confirm the efficacy of ACLY inhibition *in vivo*, siRNA oligo with atelocollagen was injected into A549 cell xenografts in nude mice. ACLY siRNA treatment significantly inhibited tumor growth ($P < 0.0001$; Fig. 5*A*) and enhanced gland formation of A549 cells (Fig. 5*B, arrows*), whereas no significant weight loss or other toxicity was observed in both groups (data not shown). It should be noted that loss of p-ACLY and Ki-67 expression was confined to the glandular structures of A549 cells, suggesting ACLY is involved in tumor differentiation and proliferation (Fig. 5*B, arrows*).

Discussion

Metabolic changes are commonly observed in malignant cells. In the 1920s, Otto Warburg (19) discovered that cancer cells displayed high aerobic glycolysis, in contrast to normal cells. It was further found that cancers derive most fatty acids from *de novo* synthesis (20). Although the ultimate reasons for high glycolysis and lipogenesis in cancer cells are not completely understood, it seems that cancer cells can coordinate the related metabolic enzymes and can use all products effectively.

ACLY is the first key enzyme of lipogenesis and a crosslink between glucose and lipid metabolism. ACLY overexpression or activation have been reported in urinary bladder, breast, liver, stomach, colon, and prostate tumors (21–26). However, to the best of our knowledge, this is the first observation of ACLY activation in lung cancer.

It has been reported that ACLY activity is regulated by the PI3K-Akt signaling pathway through the phosphorylation (11, 27). Akt also up-regulates ACLY mRNA levels via activation of SREBP-1, a transcription factor of cholesterol and fatty acid biosynthesis (28, 29). We observed a positive correlation among mRNA, total protein, and phosphorylated protein levels of ACLY in lung

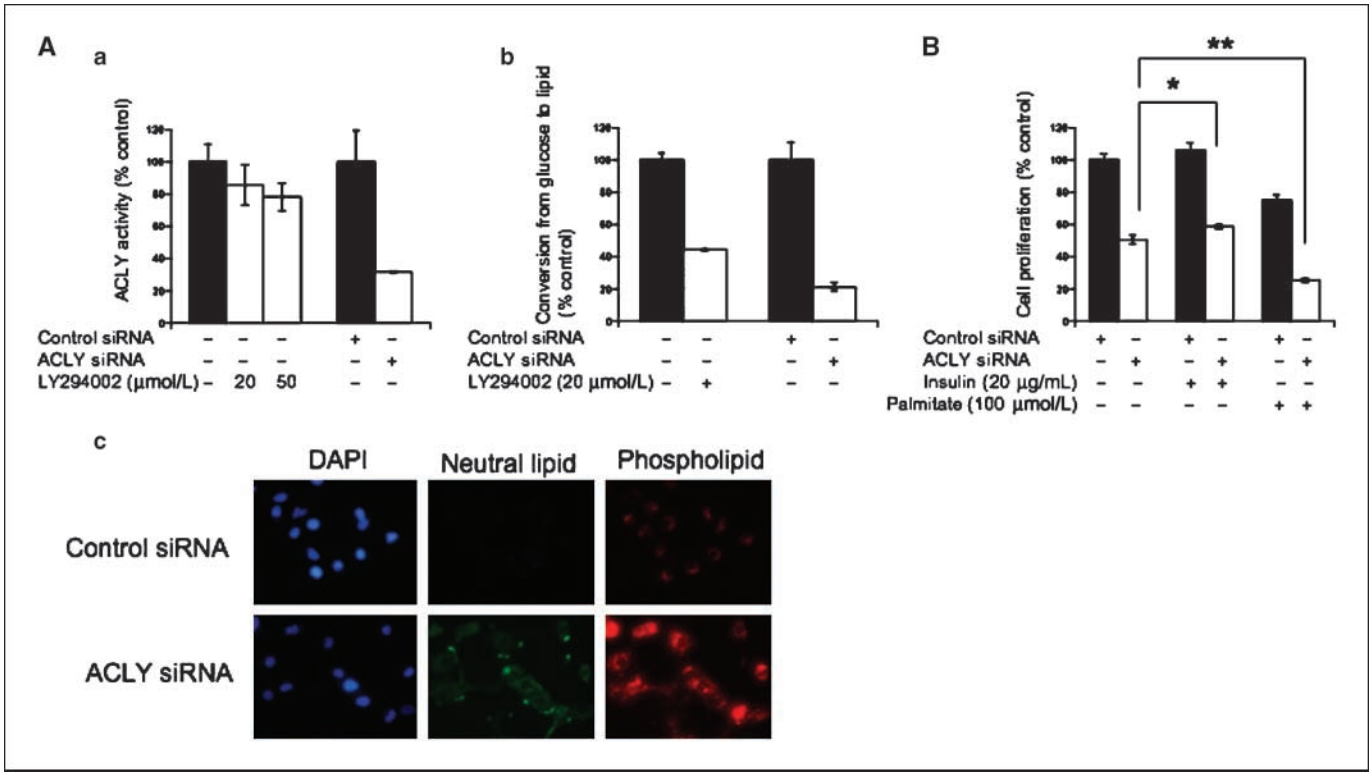

Figure 4. ACLY inhibition impairs glucose and lipid metabolism in A549 cells. *A,* ACLY inhibition changes lipid metabolism. *a,* ACLY activity assay was performed under the treatment of LY294002 or siRNA. The treatment of LY294002 or ACLY siRNA significantly reduced ACLY activity compared with control ($P < 0.05$ and $P < 0.005$, respectively). *b,* conversion rate of glucose to lipid was measured with ^{14}C-glucose under the treatment of LY294002 or siRNA. *c,* intracellular lipid accumulation was assessed using lipids conjugated to fluorescent dyes. ACLY knockdown stimulates the incorporation of extralipids. *B,* exogenous palmitate does not rescue the growth arrest induced by ACLY inhibition. Cell proliferation was measured 72 h after siRNA treatment. Cells were also treated for 24 h in the presence of 20 μg/mL insulin or 100 μmol/L palmitate-BSA complex. *, $P < 0.005$. **, $P < 0.001$. *Columns,* means; *bars,* SD.

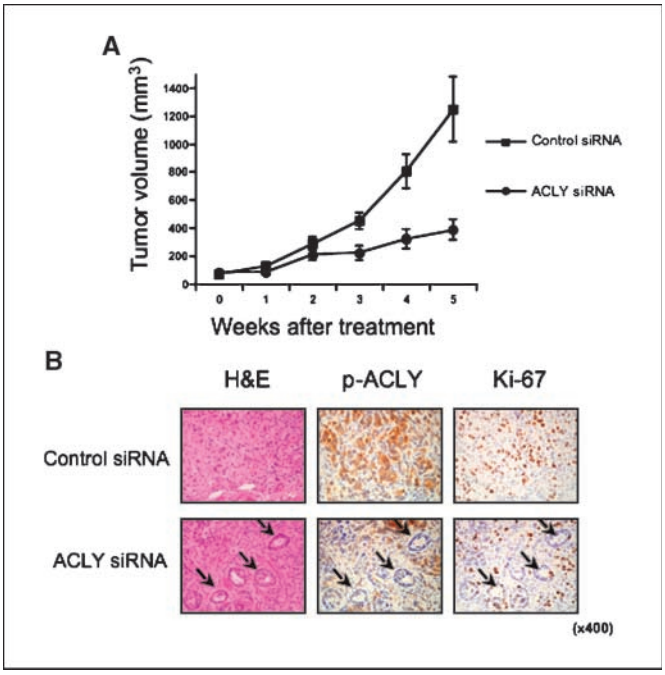

Figure 5. siRNA against ACLY inhibits tumor growth *in vivo*. A549 cells were inoculated s.c. in 20 nude mice and were allowed to grow for 10 d. Then, mice were divided into 2 groups, and ACLY siRNA#1 or negative control siRNA were injected into the tumors at weekly intervals for 5 wk. *A,* tumor growth curves in nude mice. ACLY siRNA (5 μmol/L) or the negative control siRNA (5 μmol/L) were mixed with atelocollagen, and a 200 μL aliquot of either mixture was injected into the tumor region. Tumor diameters and body weight were measured at weekly intervals and tumor volumes were calculated. *Points,* mean (n = 10 tumors per group); *bars,* SE. Significant difference curves were evaluated by an exponential regression analysis ($P < 0.0001$). *B,* H&E staining and IHC of p-ACLY and Ki-67 in A549 xenografts treated with siRNA. Note the decrease of p-ACLY and Ki-67 expression in glands (*arrows*) of A549 cells treated with ACLY siRNA.

adenocarcinoma cell lines and clinical samples. However, ACLY protein levels were independent of SREBP-1, and there was an inverse relationship between mRNA of ACLY and SREBP-1, consistent with previous reports (30, 31). Thus, activation of the PI3K-Akt pathway may stimulate ACLY activity predominantly through its phosphorylation rather than transcriptional up-regulation and, may in part, contribute to protein stabilization.

ACLY can be phosphorylated at different site by other kinase such as nucleoside diphosphate kinase (32) and cyclic AMP-dependent protein kinase (33). Our study showed that despite the treatment of PI3K inhibitors resulted in the rapid and the sufficient dephosphorylation of Akt, it did the dephosphorylation of ACLY with less efficiency. Furthermore, ACLY activity was also decreased with the treatment of PI3K inhibitors, but its effect on activity was not as great as that of ACLY knockdown. Therefore, this suggested that ACLY activity is also regulated by other than PI3K-Akt pathway in lung cancer.

ACLY is considered to be localized in the cytoplasm and generates cytosolic acetyl-CoA from citrate. However, we observed the nuclear and cytoplasmic localization of ACLY protein in cell lines as well as in clinical samples. ACLY as a nuclear phosphoprotein has been shown in HeLa cells (34), but the function of nuclear ACLY remains to be elucidated. Further study is required to understand the molecular basis of differential ACLY subcellular localization.

Recent evidence suggests that dysregulated lipogenesis plays a causal role in cancer pathogenesis (35). FASN, which is a downstream *de novo* lipogenic enzyme of ACLY, is frequently overexpressed in many cancers. Interestingly, the genes of key lipogenic enzymes including acetyl-CoA carboxylase (ACC), FASN, and ACLY are all located at the 17q chromosome, and gene amplification has been reported in prostate cancer (36). Importantly, inhibition of FASN induces apoptosis in a variety of cancer cells concomitant with the decrease in phospholipids (37, 38). Supplementation of palmitate, which is the fatty acid generated by FASN, rescues apoptosis induced by ACC or FASN inhibition (39–41). To investigate potential mechanisms for the growth arrest induce by ACLY inhibition, we assessed *de novo* lipogenesis and cell proliferation in an ACLY knockdown model. First, the conversion rate from glucose to lipid was dramatically decreased by ACLY knockdown concomitant with the decrease in cell proliferation. Next, we found that the intracellular lipid levels were increased by ACLY knockdown, albeit *de novo* synthesis was impaired. Finally, the supplementation of insulin could improve cell proliferation; however, palmitate induced cell death in these cells. Taken all together, it is tempting to speculate that ACLY inhibition may affect cell proliferation due to the impairment of glucose metabolism rather than due to the depletion of lipid products generated by fatty acids or cholesterol synthesis. Because ACLY integrates glucose metabolism with lipid synthesis, ACLY inactivation could potentially affect not only lipid metabolism but also glucose metabolism. Our data showed that ACLY inhibition, unlike FASN or ACC inhibition, lead to proliferation arrest but not apoptosis. One possible mechanism is that the salvage of extracellular lipids can prevent cell death. The precise mechanism of lipid accumulation induced by ACLY inhibition will require further study.

Importantly, p-ACLY overexpression was significantly correlated with tumor differentiation and poorer prognosis in our cohort. Because all patients enrolled in this study were operable with a relatively early stage, ACLY can be a useful marker for the identification of early-stage tumors with poorer prognosis. Besides, given that *in vivo* treatment with ACLY siRNA inhibited tumor growth in xenograft model, ACLY can be an attractive target for RNA interference therapy in the clinical setting.

There is a growing realization that signaling abnormalities within nutrient signaling pathways, for example loss-of-function mutations in the LKB1, TSC, and PTEN, can lead to transformation and tumor progression (42). Cancer cells need to obtain high energy and macromolecules effectively. Because ACLY integrates between glycolytic and lipogenic process, it may be important for the coordination of cancer cell metabolism.

Recent cancer research has highlighted the importance of lipid metabolism in cancer cells (35, 43). The present study provided a solid link between a metabolic network and lung cancer pathogenesis. We believe research into ACLY will open up opportunities for identifying new drugs for treatment of this deadly disease as well as other types of malignant tumors.

Disclosure of Potential Conflicts of Interest

No potential conflicts of interest were disclosed.

Acknowledgments

Received 4/7/2008; revised 7/23/2008; accepted 8/4/2008.

Grant support: Parts of this study was supported financially by Grants-in-Aid for Scientific Research on Priority Areas from the Ministry of Education, Culture, Sports, Science and Technology; Grants-in-Aid for Scientific Research from the Japan Society for the Promotion of Science; and by grants from the Ministry of Health, Labour and Welfare, the National Institute of Biomedical Innovation, the Smoking Research Foundation, and the Vehicle Racing Commemorative Foundation.

The costs of publication of this article were defrayed in part by the payment of page charges. This article must therefore be hereby marked *advertisement* in accordance with 18 U.S.C. Section 1734 solely to indicate this fact.

We thank Tomoyo Kakita and Hironori Murayama for their excellent technical assistance, and Savyon Cohen, Jonathan Cohen, and Dr. Malcolm Moore for editing the manuscript.

References

1. Elstrom RL, Bauer DE, Buzzai M, et al. Akt stimulates aerobic glycolysis in cancer cells. Cancer Res 2004;64:3892–9.
2. Fresno Vara JA, Casado E, de Castro J, Cejas P, Belda-Iniesta C, Gonzalez-Baron M. PI3K/Akt signalling pathway and cancer. Cancer Treat Rev 2004;30:193–204.
3. Whiteman EL, Cho H, Birnbaum MJ. Role of Akt/protein kinase B in metabolism. Trends Endocrinol Metab 2002;13:444–51.
4. Coleman RE. PET in lung cancer. J Nucl Med 1999;40:814–20.
5. Higashi K, Ueda Y, Matsunari I, et al. 11C-acetate PET imaging of lung cancer: comparison with 18F-FDG PET and 99mTc-MIBI SPET. Eur J Nucl Med Mol Imaging 2004;31:13–21.
6. Pelicano H, Martin DS, Xu RH, Huang P. Glycolysis inhibition for anticancer treatment. Oncogene 2006;25:4633–46.
7. Swinnen JV, Brusselmans K, Verhoeven G. Increased lipogenesis in cancer cells: new players, novel targets. Curr Opin Clin Nutr Metab Care 2006;9:358–65.
8. Gatenby RA, Gillies RJ. Glycolysis in cancer: a potential target for therapy. Int J Biochem Cell Biol 2007;39:1358–66.
9. Ko YH, Smith BL, Wang Y, et al. Advanced cancers: eradication in all cases using 3-bromopyruvate therapy to deplete ATP. Biochem Biophys Res Commun 2004;324:269–75.
10. Brown AJ. Cholesterol, statins and cancer. Clin Exp Pharmacol Physiol 2007;34:135–41.
11. Berwick DC, Hers I, Heesom KJ, Moule SK, Tavare JM. The identification of ATP-citrate lyase as a protein kinase B (Akt) substrate in primary adipocytes. J Biol Chem 2002;277:33895–900.
12. Bauer DE, Hatzivassiliou G, Zhao F, Andreadis C, Thompson CB. ATP citrate lyase is an important component of cell growth and transformation. Oncogene 2005;24:6314–22.
13. Hatzivassiliou G, Zhao F, Bauer DE, et al. ATP citrate lyase inhibition can suppress tumor cell growth. Cancer Cell 2005;8:311–21.
14. Travis WD CT, Corrin B, Shimosato Y, Brambilla E. Histological Typing of Lung and Pleural Tumors: World Health Organization International Histological Classification of Tumors. 3rd ed. Berlin: Springer; 1999.
15. Srere PA. The citrate cleavage enzyme. I. Distribution and purification. J Biol Chem 1959;234:2544–7.
16. Brusselmans K, Vrolix R, Verhoeven G, Swinnen JV. Induction of cancer cell apoptosis by flavonoids is associated with their ability to inhibit fatty acid synthase activity. J Biol Chem 2005;280:5636–45.
17. Bligh EG, Dyer WJ. A rapid method of total lipid extraction and purification. Can J Biochem Physiol 1959;37:911–7.
18. Team RDC. R: A language and environment for statistical computing. 2007 cited; Available from: http://www.R-project.org.
19. Warburg O. On the origin of cancer cells. Science 1956;123:309–14.
20. Medes G, Thomas A, Weinhouse S. Metabolism of neoplastic tissue. IV. A study of lipid synthesis in neoplastic tissue slices *in vitro*. Cancer Res 1953;13:27–9.
21. Turyn J, Schlichtholz B, Dettlaff-Pokora A, et al. Increased activity of glycerol 3-phosphate dehydrogenase and other lipogenic enzymes in human bladder cancer. Horm Metab Res 2003;35:565–9.
22. Szutowicz A, Kwiatkowski J, Angielski S. Lipogenetic and glycolytic enzyme activities in carcinoma and nonmalignant diseases of the human breast. Br J Cancer 1979;39:681–7.
23. Yahagi N, Shimano H, Hasegawa K, et al. Co-ordinate activation of lipogenic enzymes in hepatocellular carcinoma. Eur J Cancer 2005;41:1316–22.
24. Yancy HF, Mason JA, Peters S, et al. Metastatic progression and gene expression between breast cancer cell lines from African American and Caucasian women. J Carcinog 2007;6:8.
25. Varis A, Wolf M, Monni O, et al. Targets of gene amplification and overexpression at 17q in gastric cancer. Cancer Res 2002;62:2625–9.
26. Halliday KR, Fenoglio-Preiser C, Sillerud LO. Differentiation of human tumors from nonmalignant tissue by natural-abundance 13C NMR spectroscopy. Magn Reson Med 1988;7:384–411.
27. Manning BD, Cantley LC. AKT/PKB signaling: navigating downstream. Cell 2007;129:1261–74.
28. Sato R, Okamoto A, Inoue J, et al. Transcriptional regulation of the ATP citrate-lyase gene by sterol regulatory element-binding proteins. J Biol Chem 2000;275:12497–502.
29. Porstmann T, Griffiths B, Chung YL, et al. PKB/Akt induces transcription of enzymes involved in cholesterol and fatty acid biosynthesis via activation of SREBP. Oncogene 2005;24:6465–81.
30. Rebouissou S, Imbeaud S, Balabaud C, et al. HNF1α inactivation promotes lipogenesis in human hepatocellular adenoma independently of SREBP-1 and carbohydrate-response element-binding protein (ChREBP) activation. J Biol Chem 2007;282:14437–46.
31. Goldstein JL, Rawson RB, Brown MS. Mutant mammalian cells as tools to delineate the sterol regulatory element-binding protein pathway for feedback regulation of lipid synthesis. Arch Biochem Biophys 2002;397:139–48.
32. Wagner PD, Vu ND. Phosphorylation of ATP-citrate lyase by nucleoside diphosphate kinase. J Biol Chem 1995;270:21758–64.
33. Pierce MW, Palmer JL, Keutmann HT, Avruch J. ATP-citrate lyase. Structure of a tryptic peptide containing the phosphorylation site directed by glucagon and the cAMP-dependent protein kinase. J Biol Chem 1981;256:8867–70.
34. Beausoleil SA, Jedrychowski M, Schwartz D, et al. Large-scale characterization of HeLa cell nuclear phosphoproteins. Proc Natl Acad Sci U S A 2004;101:12130–5.
35. Menendez JA, Lupu R. Fatty acid synthase and the lipogenic phenotype in cancer pathogenesis. Nat Rev Cancer 2007;7:763–77.
36. Shah US, Dhir R, Gollin SM, et al. Fatty acid synthase gene overexpression and copy number gain in prostate adenocarcinoma. Hum Pathol 2006;37:401–9.
37. De Schrijver E, Brusselmans K, Heyns W, Verhoeven G, Swinnen JV. RNA interference-mediated silencing of the fatty acid synthase gene attenuates growth and induces morphological changes and apoptosis of LNCaP prostate cancer cells. Cancer Res 2003;63:3799–804.
38. Zhou W, Simpson PJ, McFadden JM, et al. Fatty acid synthase inhibition triggers apoptosis during S phase in human cancer cells. Cancer Res 2003;63:7330–7.
39. Kuhajda FP, Jenner K, Wood FD, et al. Fatty acid synthesis: a potential selective target for antineoplastic therapy. Proc Natl Acad Sci U S A 1994;91:6379–83.
40. Kridel SJ, Axelrod F, Rozenkrantz N, Smith JW. Orlistat is a novel inhibitor of fatty acid synthase with antitumor activity. Cancer Res 2004;64:2070–5.
41. Chajes V, Cambot M, Moreau K, Lenoir GM, Joulin V. Acetyl-CoA carboxylase α is essential to breast cancer cell survival. Cancer Res 2006;66:5287–94.
42. Marshall S. Role of insulin, adipocyte hormones, and nutrient-sensing pathways in regulating fuel metabolism and energy homeostasis: a nutritional perspective of diabetes, obesity, and cancer. Sci STKE 2006;2006:re7.
43. Deberardinis RJ, Lum JJ, Hatzivassiliou G, Thompson CB. The biology of cancer: metabolic reprogramming fuels cell growth and proliferation. Cell Metab 2008;7:11–20.